

Synthesis and Conformational Properties of the Lanthionine-Bridged Opioid Peptide [D-Ala^L₂,Ala^L₅]enkephalin As Determined by NMR and Computer Simulations

Alexander Polinsky, Michael G. Cooney, Anna Toy-Palmer, George Ósabay, and Murray Goodman*

Department of Chemistry, University of California, San Diego, La Jolla, California 92093

Received November 14, 1991

We report the synthesis and conformational analysis by means of NMR and computer simulations of a novel opioid peptide with the sequence H-Tyr-NH-CH-CO-Gly-Phe-NH-CH-CONH₂, which

we write as H-Tyr-[D-Ala^L₂-Gly-Phe-Ala^L₅]-NH₂, abbreviated [D-Ala^L₂,L-Ala^L₅]EA, where Ala^L denotes each of the lanthionine amino acid ends linked by a monosulfide bridge and EA indicates enkephalinamide. Data from 2D NMR (HOHAHA and ROESY) provide short-range NOEs that are used as constraints in molecular modeling; measurement of coupling constants shows that χ^1 (D-Ala^L₂) is predominantly in either the *t* or *g* conformation, and temperature coefficient data suggest the participation of the Ala^L₅ amide proton in an intramolecular hydrogen bond. The use of NOE and hydrogen-bond constraints in a distance-geometry program yields a large number of initial conformations compatible with the data. Energy minimization of these structures using CHARMM results in three families of backbone ring conformations, labeled A1, A2, and B. The torsion χ^1 in D-Ala^L₂ remains close to trans for all three conformations. Molecular dynamics in vacuo at 300 K show that these three families of conformers interconvert, with concerted shifts in two of the three torsions ψ (Phe), ϕ (Ala^L₅), and χ (Ala^L₅). The [D-Ala^L₂,L-Ala^L₅]EA is superactive in the guinea pig ileum (GPI) and mouse vas deferens (MVD) in vitro tests and also in the rat hot plate test in vivo. At the same time, this analog with a constrained 13-membered ring shows virtually no selectivity with a ratio IC₅₀ (MVD)/IC₅₀ (GPI) of 0.882.

Introduction

Since the discovery of the natural, endogenous enkephalins and their receptors in the mammalian brain and intestine, several classes of opioids have been discovered and various analogs synthesized: the enkephalins, based on the endogenous enkephalin sequences H-Tyr-Gly-Gly-Phe-Leu/Met; the dermorphins,¹ with prototypic formula H-Tyr-D-Ala-Phe-Gly-Tyr-Pro-Ser-NH₂; and the morphiceptins,² based on H-Tyr-Pro-Phe-Pro-NH₂. The existence of at least three classes of opiate receptors is well established at this time. These are the μ receptors, at which morphine is most active, the δ or enkephalin receptor, and the κ or dynorphin receptor. Some naturally occurring opioids display marked receptor selectivity, for example [Leu⁵]enkephalin which is δ -selective, but because of their linearity these endogenous molecules are too flexible for rigorous conformational studies. Conformationally constrained cyclic analogs widely used in peptide structure-activity studies³ have therefore been synthesized and studied in the hope of elucidating the critical residues or portions of the molecule for opiate receptor binding. Some topological features of the opiate receptors themselves may be revealed after key structure-function relationships for their ligands have been elucidated.

In the past decade many such cyclic opioids have been synthesized, tested for activity, and subjected to structural analysis by NMR and computer simulations. Some of these are cyclized via backbone to side chain, while others have the two side chains of residues 2 and 5 joined to form a disulfide bridge. The first cyclic analog was synthesized and studied by Schiller⁴ and has the sequence H-Tyr-c-[D-A₂bu-Gly-Phe-Leu], where A₂bu represents α,γ -diaminobutyric acid, with the backbone of Leu joined to the side chain of A₂bu. We have carried out numerous studies of conformational properties of this parent cyclic enkephalin and related analogs; incorporation of retro-inverso modifications in different positions of the backbone and conformational analysis of the resulting compounds allowed the study of the role of the backbone in potency and selectivity.^{5,6} It was found that μ -selective analogs such as H-Tyr-c-[D-A₂bu-Gly-Phe-Leu] are constrained and prefer the tyrosine and phenylalanine rings far part in an extended conformation. Reversal of the Leu backbone chirality, however, increases the flexibility and results in nonselective receptor binding; a retro-inverso modification of the backbone between Phe and Leu to H-Tyr-c-[D-A₂bu-Gly-*g*Phe-*R-m*Leu], where *g* indicates a *gem*-diaminoalkyl residue and *m* represents a malonyl residue, also decreases selectivity.⁷

* To whom correspondence should be addressed.

(1) Erspamer, V.; Melchiorri, P. Amphibian skin peptides and mammalian neuropeptides. In *Growth Hormone and Other Biologically Active Peptides*; Peclle, A., Muller, E. E., Eds.; Excerpta Medica: Amsterdam, 1980; pp 185-200.

(2) Chang, K.-J.; Killian, A.; Hazum, E.; Cautrecasas, P.; Chang, J.-K. Morphiceptin: a potent and specific agonist for morphin (μ) receptors. *Science* 1981, 212, 75-77.

(3) Hruby, V. J. Conformational Restrictions of biologically active peptides via amino acid side chain groups. *Life Sci.* 1982, 31, 189-199.

(4) Schiller, P. W. Conformational analysis of opioid peptides and the use of conformational restriction in the design of selective analogs. In *Opioid Peptides: Medicinal Chemistry*; Rapaka, R. S., Barnett, G., Hawks, R. L., Eds.; NIDA Research Monograph 1969, 1986; pp 291-311.

(5) Goodman, M.; Chorev, M. The synthesis and conformational analysis of retro-inverso analogs of biologically active molecules. In *Perspectives in Peptide Chemistry*; Eberle, A., Geiger, R., Wieland, T., Eds.; S. Karger: Basel, 1981; pp 283-293.

(6) Hassan, M.; Goodman, M. Computer simulations of cyclic enkephalin analogs. *Biochemistry* 1986, 25, 7596-7606.

Hruby⁸ and Mosberg⁹ investigated a different class of opioid peptidomimetics cyclized via a disulfide bridge. The most interesting compound in this series is DPDPE, with the composition H-Tyr-c-[D-Pen-Gly-Phe-D-Pen]-OH, where "Pen" represents penicillamine. The study by Hruby et al.⁸ reports a slightly different conformation for DPDPE from the work by Mosberg et al.⁹ However, the two models share the common features of overall rigidity and close proximity of the aromatic Tyr and Phe rings, though the Hruby model has the rings closer together. The molecule DPDPE is found to be highly δ -selective in vitro, while the more flexible DCLCE, the D-Cys²,L-Cys⁵ amide analog of DPDPE, has been found to be nonselective.¹⁰

These observations have led to the working hypothesis that μ - vs δ -selectivity of constrained opioids is directly related to the distance between the aromatic side chain rings of residues 1 and 4. Very recently, Nikiforovich et al.¹¹ has proposed alternative models for a single " μ -bound" and two " δ -bound" conformations of cyclic enkephalin analogs containing cysteines or penicillamines at positions 2 and 5 that are joined by a disulfide bridge. Interestingly, the Nikiforovich model has the δ -bound conformations more extended, with γ -like turns around Gly, than the μ -bound conformation which has a β -I-type bend around Gly and Phe. One main question remains as to whether flexibility alone determines biological potency and selectivity, and if so, which portions of the ring and which side chains are critical for such selectivity and potency.

We have designed and synthesized a representative of the new class of enkephalin analogs with a lanthionine (monosulfide) bridge, between residues 2 and 5. The ring size in these new analogs is reduced to 13 atoms as compared to 14 in DPDPE and its cysteine analogs, resulting in more conformationally constrained molecules. Lanthionine bridges exist in naturally occurring "lantibiotics" such as nisin, subtilin, and epidermin.¹²

The lanthionine bridged enkephalin analog that we have chosen for our initial studies is formulated as H-Tyr-[D-Ala_L-Gly-Phe-Ala_L]-NH₂, abbreviated [D-Ala_L²,L-Ala_L⁵]EA (for enkephalinamide). Its chemical structure, shown in Figure 1, is similar to that of DPDPE and DPLPE, but the cyclic structure contains 13 instead of 14 atoms and the lanthionine β -carbons are not methylated. Since four

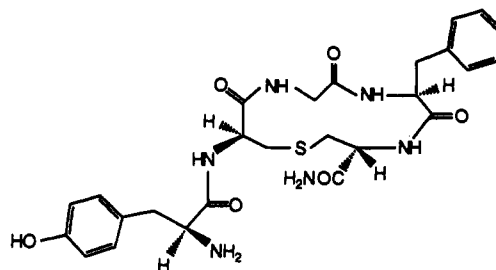


Figure 1. Chemical structure of H-Tyr-[D-Ala_L-Gly-Phe-Ala_L]-NH₂, abbreviated [D-Ala_L²,L-Ala_L⁵]EA. Note the similarity of this molecule to disulfide-bridged analogs such as DPDPE and DCLCE (see text).

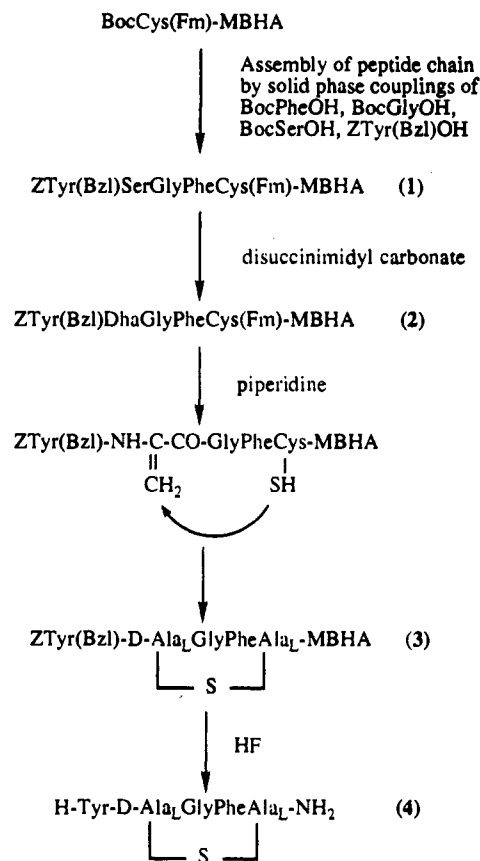


Figure 2. Scheme employed for the solid phase synthesis of [D-Ala_L²,L-Ala_L⁵]EA. See text for explanation of abbreviations.

previously tested analogs with penicillamine and cysteine,⁹ [D-Cys²,Cys⁵]EA, [D-Cys²,D-Cys⁵]EA, [D-Pen²,Cys⁵]EA, and [D-Pen²,D-Cys⁵]EA, have amidated carboxyl termini, we thought it appropriate to begin our investigations with the amide derivative.

Experimental Section

Peptide Synthesis. Three synthetic methods for the preparation of lanthionine-bridged peptides have been reviewed in a recent paper by Shiba et al.¹³ For the preparation of [D-Ala_L²,L-Ala_L⁵]EA we have selected the method that most closely simulates the biosynthesis of lanthionine peptides. The sulfide bridge was formed by the addition of the cysteine-5 SH group to the double bond of dehydroalanine-2 (Dha) on the resin. Here we describe a practical one-vessel synthesis for *meso*-lanthionine peptides on a methylbenzhydrylamine (MBHA) resin (Figure 2).

The linear peptide chain was assembled on an MBHA resin using *tert*-butoxycarbonyl (Boc) chemistry with the symmetrical

(7) Mierke, D. F.; Lucietto, P.; Goodman, M. Conformational studies of diastereomeric cyclic enkephalins by H-NMR and computer simulations. *Biopolymers* 1987, 26, 1573-1586.

(8) Hruby, V. J.; Kao, L.-F.; Pettitt, B. M.; Karplus, M. The conformational properties of the delta opioid peptide [D-Pen²,D-Pen⁵]enkephalin in aqueous solution determined by NMR and energy minimization calculations. *J. Am. Chem. Soc.* 1988, 110, 3351-3359.

(9) Mosberg, H. I.; Sobczyk-Kojiro, K.; Subramanian, P.; Crippen, G. M.; Ramalingam, K.; Woodard, R. W. Combined use of stereospecific deuteration, NMR, distance geometry, and energy minimization for the conformational analysis of the highly delta-opioid receptor selective peptide [D-Pen²,D-Pen⁵]enkephalin. *J. Am. Chem. Soc.* 1990, 112, 822-829.

(10) Mosberg, H. I.; Hurst, R.; Hruby, V. J.; Galligan, J. J.; Burks, T. F.; Gee, K.; Yamamura, H. I. Conformationally constrained cyclic enkephalin analogs with pronounced delta opioid receptor agonist selectivity. *Life Sci.* 1983, 32, 2565-2569.

(11) Nikiforovich, G. V.; Golbraikh, A. A.; Shenderovich, M. D.; Balodis, J. Conformational features responsible for the binding of cyclic analogues of enkephalin to opioid receptors. II. Models of mu- and delta-receptor-bound structures for analogues containing Phe4. *Int. J. Peptide Prot. Res.* 1990, 36, 209-218.

(12) Jung, G. Peptides with sulfide bridges and dehydroamino acids: Their prepeptides and possibilities for bioengineering. In *Peptides. Proceedings of the Eleventh American Peptide Symposium*; Rivier, J. E., Marshall, G. R., Eds.; ESCOM: Leiden, 1990; pp 865-869.

(13) Shiba, T.; Wakamiya, T.; Fukase, K.; Sano, A.; Shimbo, K.; Ueki, Y. Chemistry of lanthionine peptides. *Biopolymers* 1986, 25, S11-19.

anhydride peptide coupling method. Serine was incorporated at position 2 and then converted to dehydroalanine using *N,N'*-disuccinimidyl carbonate (DSC).¹⁴ The S-protecting fluorenyl methyl (Fm) group was selectively removed with piperidine.¹⁵ A slightly basic milieu (5% piperidine/DMF) promoted the Michael addition of the SH group to the double bond. Amino acid analysis showed a 48% conversion of serine, and probably a greater excess of the reagent DSC would result in an increased yield for these two steps. "Low-high HF cleavage" was used to cleave the peptide from the resin and to remove the protecting groups: benzyl (Bzl) and benzyloxycarbonyl (Z). Purification of the resultant crude product was achieved by preparative RP-HPLC using gradient acetonitrile/water elution. The material obtained was further purified and desalted by gel filtration on a Sephadex G-15 column (20% active acid/water).

The product was identified by amino acid analysis and mass spectrometry. Although Michael additions are not normally stereoselective, only one diastereomer was obtained. The second diastereomer could not be detected in the reaction mixture. To ascertain the stereochemistry of the product, [D-Ala²,L-Ala⁵]EA and [L-Ala²,L-Ala⁵]EA were synthesized by other unambiguous routes¹⁶ which preserve the chiralities of the lanthionine moieties. The 2D NMR analyses of the initial product and [D-Ala²,L-Ala⁵]EA were essentially identical, demonstrating that the initial product was [D-Ala²,L-Ala⁵]EA. In addition, the biological assays of both the initial product and [D-Ala²,L-Ala⁵]EA gave similar activities, thus confirming the identity of the initial product as [D-Ala²,L-Ala⁵]EA. The sterically hindering solid support adjacent to the SH group may be responsible for the stereoselectivity of this addition reaction.

Our solid-phase synthetic approach appears ideally suited to a rapid assembly of lanthionine-bridged cyclopeptides.

Experimental Procedures. All amino acids were of the L configuration except as indicated. Protected amino acids were purchased from Bachem. ACS-grade solvents (DCM, DMF, acetonitrile) were purchased from Fisher Scientific, purged with nitrogen, and then stored over molecular sieves from Sigma. *N,N'*-Diisopropylethylamine (DIEA) (Aldrich) was dried over KOH and distilled from ninhydrin. MBHA resin-HCl (Calbiochem) was swollen in dichloromethane (DCM) and washed with 5% DIEA/DCM followed by DCM before use. Trifluoroacetic acid (TFA), piperidine, DSC (Aldrich), and *N,N'*-dicyclohexylcarbodiimide (DCC) (Fluka) was used without further purification. Silica gel for flash chromatography was purchased from Baker.

Peptides were analyzed on precoated silica gel 60F-254 plates (Merck) using (A) chloroform/methanol/acetic acid, 65:35:1, (B) butanol/acetic acid/water, 4:1:5 (upper phase). Compounds were visualized by UV, ninhydrin, chlorine/*o*-toluidine, and KMnO₄ solution. RP-HPLC analyses were performed on a Waters (510 pumps, 484 detector) System with a C-18 analytical column.

Amino acid analyses were performed at the Department of Immunology of the Scripps Clinic and Research Foundation, and mass spectrometric analysis was carried out at the University of California, Riverside Mass Spectrometry Laboratory.

Preparation of Z-Tyr(Bzl)-Ser-Gly-Phe-Cys(Fm)-MBHA (1). Methylbenzhydrylamine resin (3 g) was reacted with Boc-Cys(Fm)OH (1.0 g, 2.5 mmol) and DCC (0.52 g, 2.5 mmol) in DCM (30 mL) for 3 h at room temperature in an SPPS vessel. The remaining amino groups were capped by acetylation. The resulting Boc-Cys(Fm)-MBHA resin (substitution level 0.36 mmol/g, based on picric acid titration¹⁷) was then deprotected with 30% TFA/DCM (v/v) and neutralized with 1% DIEA/DCM (v/v) solution. The peptide chain was then assembled by consecutive addition of the symmetrical anhydrides (2.5 equiv) of BocPheOH, BocGlyOH, BocSerOH, and Z-Tyr(Bzl)OH as well as deprotection steps. The completeness of coupling was

Table I. Chemical Shifts for [D-Ala²,L-Ala⁵]EA^a

	Tyr	D-Ala ²	Gly	Phe	Ala ⁵
NH	8.10	8.73	8.82	8.25	7.26
H _α	3.93	4.54	4.05 3.23	4.56	4.29
H _β	2.85	2.61 2.35		3.12 2.83	2.92
H _{ar} (ortho)	7.00			7.24	
H _{ar} (meta)	6.70			7.25	
H _{ar} (para)				7.25	
H _{OH}	9.36				
CONH ₂					7.20 7.46

^a All values in ppm.

monitored by the Kaiser test.¹⁸ Coupling of Z-Tyr(Bzl)OH was repeated with 1 molar equiv of reagent. Yield: 1.06 mmol (84%) peptide based on Gly. Amino acid analysis: Cys₍₁₎Gly_{1.00}Phe_{0.86}Ser_{1.42}Tyr_{1.22}.

Preparation of Z-Tyr(Bzl)-c-(D-Ala¹-Gly-Phe-Ala¹)-MBHA (3). The protected peptidyl MBHA resin (1, 1.06 mmol) in the SPPS vessel was swollen and then suspended in DCM (20 mL). A solution of DSC (387 mg, 1.51 mmol) in acetonitrile (10 mL) was added to the reaction mixture followed by a 5% DIEA/DCM solution (5.22 mL, 1.5 mmol of DIEA). The reaction was allowed to proceed for 4 h, with shaking at room temperature in a nitrogen atmosphere. The reaction mixture was drained, and the solid phase was washed with DCM (4×). The product (2) was treated with a solution of 20% piperidine/DMF solution (20 mL, v/v, 2 × 50 min) and shaken in a 5% piperidine/DMF-DCM solution (40 mL, 1/1, v/v) overnight. The solution phase was drained, and the resin was washed with DMF (1×), DCM (2×), and EtOH (2×) and dried. Yield: 3.7 g.

Preparation of H-Tyr(D-Ala¹-Gly-Phe-Ala¹)-NH₂ or [D-Ala²,L-Ala⁵]EA (4). The peptidyl resin 3 (1.0 g) was treated with anhydrous HF (20 mL) at 0 °C in the presence of anisole (1 mL) for 1 h in a Teflon HF apparatus. After removal of volatile components, the remaining material was washed with ethyl acetate (2 × 20 mL) and the product was extracted with acetic acid followed by 10% acetic acid/water solution. The combined extracts were lyophilized (yield 200 mg). This material was purified by preparative RP-HPLC on a Vydac C-18 column (1.0 × 25 cm) eluted with 0.1% TFA in acetonitrile/water. A linear gradient from 15% to 22% acetonitrile over 12 min with a flow rate of 10 mL/min was employed. The appropriate fractions were lyophilized to give a solid product (yield 87 mg). Finally, 30 mg of the product was subjected to gel permeation chromatography (1.5 × 100 cm Sephadex G-15 eluted with 20% acetic acid). The peptide fractions were pooled and lyophilized. Yield 16 mg (28.8 μmol, 29.1% calculated for compound 1). R_f(A) 0.44; R_f(B) 0.49. FAB-MS: *m/e* 557 (M + 1). Amino acid analysis: Gly_{1.00}Lan_{1.1}Phe_{0.99}Tyr_{0.95}. ¹H NMR data are presented in Table I.

Bioactivity. The assays based on inhibition of electrically induced contractions of the guinea pig ileum¹⁹ and mouse vas deferens assay²⁰ were carried out by Schiller and his associates at the Clinical Research Institute of Montreal, Canada. For the in vivo assay, a rat hot-plate test utilizing intrathecal injections was carried out by Yaksh and his co-workers²¹ at the University of California San Diego.

(18) Kaiser, E.; Colescott, R. L.; Bossinger, C. D.; Cook, P. I. Color test for detecting of free terminal amino groups in the solid phase synthesis of peptides. *Anal. Biochem.* 1970, 34, 595-598.

(19) Paton, W. The action of morphine and related substances on contraction and on acetylcholine output of coxially stimulated guinea-pig ileum. *Br. J. Pharmacol.* 1957, 12, 119-127.

(20) Henderson, G.; Hughes, J.; Kosterlitz, H. W. A new example of a morphine-sensitive neuroeffector junction: adrenergic transmission in the mouse vas deferens. *Br. J. Pharmacol.* 1972, 46, 764-766.

(21) Yaksh, T. L.; Jang, J.; Nishiuchi, Y.; Braun, K. P.; Ro, S. The utility of 2-hydroxypropyl-beta-cyclodextrin as a vehicle for the intracerebral and intrathecal administration of drugs. *Life Sci.* 1991, 48, 622-623.

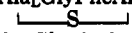
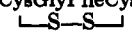
(14) Ogura, H.; Sato, O.; Takeda, K. Beta-elimination of beta-hydroxylamino acids with disuccinimidyl carbonate. *Tetrahedron. Lett.* 1981, 22, 4817-4818.

(15) Bodanszky, M.; Bednarek, M. A. Derivatives of S-9-fluoromethyl-L-cysteine. *Int. J. Pept. Protein Res.* 1982, 20, 434-437.

(16) Harpp, D. N.; Gleason, J. G. Preparation and mass spectral properties of cysteine and lanthionine derivatives. *J. Org. Chem.* 1971, 36, 73-80.

(17) Gisin, B. F. The monitoring of reactions in solid-phase peptide synthesis with picric acid. *Anal. Chim. Acta* 1972, 58, 248-249.

Table II. Inhibitory Potency and Selectivity in GPI and MVD Bioassays and Rat Hot-Plate Test in Vivo

compound	GPI		MVD		MVD/GPI	hot plate in vivo test: ED ₅₀ (μg/kg)
	IC ₅₀ (nM)	rel potency	IC ₅₀ (nM)	rel potency		
H-Tyr-D-Ala ₁ GlyPheAla ₁ -NH ₂ 	0.62	396	0.54	21	0.882	0.15
H-Tyr-D-CysGlyPheCys-NH ₂ 	1.51	132	0.76	17	0.503	
[Leu ⁶]enkephalin	246	1	11.4	1	0.046	>100
morphine	58.6 ^a	4.2	644 ^a	0.02	11	5.6

^a Salvadori, S.; et al. *Hoppe-Seyler's Z. Physiol. Chem.* 1984, 365, 1199.

The [D-Ala₁²,L-Ala₁⁵]EA is superactive in GPI and MVD in vitro tests and also in the rat hot-plate test in vivo. At the same time, this analog with a constrained 13-membered ring shows virtually no selectivity with a ratio IC₅₀ (MVD)/IC₅₀ (GPI) of 0.882 (Table II).

NMR Measurements. All ¹H NMR spectra were measured on a General Electric GN-500 spectrometer operating at 500 MHz. All experiments were carried out in DMSO-*d*₆ (MSD Isotopes) at a concentration of 1.5 mg/mL. Temperature coefficients $\tau = d\delta/dT$ were calculated from spectra collected at temperatures ranging from 25 to 50 °C. The peak assignments were made with 2D homonuclear Hartmann-Hahn experiments (HOHAHA) and 2D rotating frame NOE experiments (ROESY).

The HOHAHA experiments employed the MLEV 17 spin-locking sequence suggested by Bax.²² The time proportional phase increment method²³ was used to obtain the absolute phase. A mixing time of 75 ms with a spin-locking field of 10.2 KHz was employed.

The ROESY experiments^{24,25} were carried out using mixing times of 100–300 ms with a spin-locking field of 2 KHz employing 2D hypercomplex Fourier transformation as suggested by States et al.²⁶ and Muller and Ernst.²⁷ Gaussian multiplication and zero filling in *t*₁ were applied to result in a final set of 2K × 2K points.

Amide to α -proton *J* coupling constants were measured and ϕ torsional angles determined from one dimensional spectra^{28,29} using Cung's set of parameters.²⁹ Vicinal coupling constants around C α -C β bonds were also measured where possible and fractions of *t*, *g*⁻, and *g*⁺ conformers were calculated for χ_1 torsional angles following a procedure suggested by Yamazaki.³⁰

Computer Simulations. All calculations were performed on a Personal Iris 4D-25 workstation and IRIS 4D-340 computer (Silicon Graphics). Energy minimizations and molecular dynamics were carried out with the molecular modeling package which included QUANTA 3.0 (Molecular Simulation, Inc.) and CHARMM.^{31,32}

All hydrogen atoms were included in all calculations. The potential energy of the molecular system was expressed by the

valence force field implemented in CHARMM³¹ (without an explicit hydrogen bonding term) with the PARM30 parameter set. In molecular dynamics simulations, charges of functional groups that are normally solvated (the hydroxyl in Tyr and the C-terminal amide group) were set to zero. In addition to the solvation of these groups and their resulting unavailability for intramolecular interactions, another rationale for setting these charges to zero is that such groups themselves are not necessary for pharmacological activity. DiMaio et al.³³ showed that substitution of Phe for Tyr in cyclic analogs reduces potency but still gives an analog that is twice as potent as the linear [Leu⁶]enkephalin, and many active analogs cyclized through the backbone have also been synthesized.⁴ A distance-dependent dielectric constant ($\epsilon = R$) was used in all calculations.

Energy minimizations with respect to all the Cartesian coordinates were carried out using the Adopted Basis Newton-Raphson (ABNR) algorithm³¹ until all derivatives were smaller than 0.001 kcal/mol Å.

Molecular dynamics simulations were performed by numerical integration of Newton's equations of motion with a second-order predictor two-step Verlet algorithm.³⁴ The SHAKE algorithm³⁵ was used, which allowed a step size of 1 fs in dynamics. All simulations were preceded by 0.3 ps of heating from 0 to 300 K followed by a 2.7-ps equilibration period. Equilibrations and simulations were performed at 300 K.

Conformational Searches. The search for low-energy conformations consistent with NMR data included several steps. First, the distance-geometry method³⁶ was applied to generate a set of 400 conformations using distance constraints derived from observed NOEs (the DGEOM program by Blaney et al. was obtained through QCPE, program no. 590). Ascribing a particular interproton distance to a strong, medium or weak NOE is based on the assumption that the cross-peak intensity for a particular pair of protons depends only on the distance separating these protons. It has been shown that, even for relatively short mixing times, in multispin systems this approach systematically underestimates the distances.³⁷ With this in mind we used ranges of 2.5 Å or less (but not less than the van der Waals lower limit) for strong, 2.5–3.0 Å for medium, and 3.0–4.5 Å for weak NOEs (Figure 3), which do not correspond to the simple inverse sixth power distance dependence. Random sampling in torsion space was used for a fuller sampling of the allowed distance range between any two atoms.³⁸ The structures so generated were then energy minimized, with no constraints applied. Only confor-

(22) Bax, A.; Davis, D. G. MLEV-17-based two-dimensional homonuclear magnetization transfer spectroscopy. *J. Magn. Reson.* 1985, 65, 355.

(23) Marion, D.; Wuthrich, K. Application of phase sensitive two-dimensional correlated spectroscopy (COSY) for measurements of H-H spin coupling constants in proteins. *Biochem. Biophys. Res. Commun.* 1983, 113, 967.

(24) Bothner-By, A. A.; Stephens, R. L.; Lee, J.; Warren, C. D.; Jeanloz, R. W. Structure determination of a tetrasaccharide: transient Nuclear Overhauser effects in the rotating frame. *J. Am. Chem. Soc.* 1984, 106, 811.

(25) Bax, A.; Davis, D. G. Practical aspects of two-dimensional transverse NOE spectroscopy. *J. Magn. Reson.* 1985, 63, 207.

(26) States, D. J.; Haberkorn, R. A.; Ruben, D. J. A two-dimensional nuclear Overhauser experiment with pure absorption phase in four quadrants. *J. Magn. Reson.* 1982, 48, 286.

(27) Muller, L.; Ernst, R. R. Coherence transfer in the rotating frame. Application to heteronuclear cross-correlation spectroscopy. *Mol. Phys.* 1979, 38, 963.

(28) Bystrov, V. F. Spin-spin coupling and the conformational states of peptide systems. *Prog. NMR Spectrosc.* 1976, 10, 41–81.

(29) Cung, M. T.; Marraud, M.; Neel, J. Experimental calibration of a Karplus relationship in order to study the conformations of peptides by Nuclear Magnetic Resonance. *Macromolecules* 1974, 7, 606–613.

(30) Yamazaki, T.; Abe, A. Conformational studies of N-acetyl-N-methylamide derivatives of alpha-aminobutyric acid, norvaline, and valine. I. Preferred conformation in solution as studied by H-NMR spectroscopy. *Biopolymers* 1988, 27, 969–984.

(31) Brooks, B. R.; Brucoleri, R. E.; Olafson, B. D.; States, D. J.; Swaminathan, S.; Karplus, M. CHARMM: A program for macromolecular energy, minimization, and dynamics calculations. *J. Comp. Chem.* 1983, 4, 187.

(32) Nilson, L.; Karplus, M. Empirical energy functions for energy minimization and dynamics of nucleic acids. *J. Comp. Chem.* 1986, 7, 591.

(33) DiMaio, J.; Lemieux, C.; Schiller, P. W. Structure-activity relationships of cyclic enkephalin analogs. *Life Sci.* 1982, 31, 2253–2256.

(34) Verlet, L. Computer "experiments" on classical fluids. I Thermodynamical properties of Lennard-Jones molecules. *Phys. Rev.* 1967, 159, 98.

(35) van Gunsteren, W. F.; Berendsen, H. J. C. Algorithms for macromolecular dynamics and constraint dynamics. *Mol. Phys.* 1977, 34, 1311.

(36) Crippen, G. M.; Havel, T. F. *Distance Geometry and Molecular Conformation*; Research Studies Press: New York, 1988.

(37) Borgias, B. A.; James, T. L. A method for constrained refinement of macromolecular structure based on two-dimensional nuclear Overhauser effect spectra. *J. Magn. Reson.* 1988, 79, 493–512.

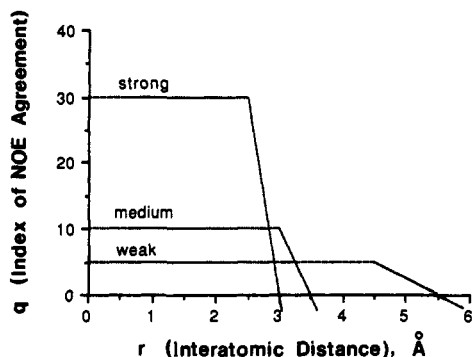


Figure 3. Graphical presentation of the NOE index scaling system discussed in the text. As is evident from the figure, the index of NOE agreement q falls far more rapidly with increasing interatomic distance for a strong NOE than for a medium or weak NOE.

mations within a 10-kcal range above the lowest energy were further analyzed. After minimization, the conformations were divided into families (clusters) based on the overall shape of their 13-membered rings.

The cluster analysis was performed as follows. First, the lowest energy conformation was extracted from the entire set of structures. This conformation served as a nucleus or seed for the first cluster. Then all structures were compared with the seed. For each of these structures, if none of the dihedral angles differed from the corresponding angles in the seed by more than a specified limiting value, that structure was added to the cluster. The threshold value used was determined empirically such that the RMS variation of any of the backbone dihedral angles of the structures comprising each cluster did not exceed 30°. After all structures were compared, the lowest energy conformation from the remaining structures were extracted and used as the nucleus of a second cluster. This process was continued until all structures were assigned to clusters. The algorithm used differs from that supplied with the standard QUANTA package in that instead of calculating the RMS differences in all torsions between two conformations, each torsion angle was compared individually.

As a final step, starting with the lowest energy conformation of each cluster, torsions external to the 13-membered ring, χ^1 (Tyr), ϕ (Ala^{L2}), and χ^1 (Phe) were varied systematically in 60° increments. The resulting new conformations were again minimized with respect to total potential energy using CHARMM as described. Again, only structures with a 10-kcal range of the lowest energy were used in the analysis.

Selection of Conformations Compatible with NMR Data. Three types of measurable parameters are available from an NMR experiment that can be used as criteria for selection. First, the presence of possible hydrogen bonds in each structure was checked using a cutoff value of 2.1 Å and compared with temperature coefficients of amide protons. Second, for each structure the ϕ torsion angles in D-Ala^{L2}, Gly, Phe, and Ala^{L5}, as well as χ^1 in D-Ala^{L2} were compared with the values calculated from observed coupling constants. Structures were selected in which no single backbone ϕ angle differed by more than 20° from its value calculated from coupling constant data.

Third, all the structures were tested for consistency with experimental NOEs. The following qualitative selection criterion was used. For each pair of protons showing an NOE the parameter q_i was calculated:

$$q_i = A \text{ for } r \leq r_0$$

$$q_i = A \left(1 - \frac{r - r_0}{r' - r_0} \right) \text{ for } r > r_0$$

where A is a scaling factor reflecting the importance of the particular NOE and r' is a distance where the parameter q_i is

equal to zero. We used values for A of 30.0, 10.0, and 5.0 for strong, medium, and weak NOEs, respectively. Values of r_0 and r' were 2.5 and 3.0 Å for strong, 3.0 and 3.5 Å for medium, and 4.5 and 5.5 Å for weak NOEs. This scaling scheme is presented graphically in Figure 3. The overall index of NOE agreement Q was calculated as a sum of q_i :

$$Q = \sum q_i$$

The use of a uniform formalized selection criterion is necessary when working with a large number of conformations. The criterion described, though qualitative in nature, reflects important intuitive requirements used in estimating the agreement of the structure with NOE data. These requirements are summarized as follows. The violation of a strong NOE should be penalized more than the violation of a weak NOE, since the presence of a strong NOE indicates unambiguously that two protons are close to each other, while a weak NOE might be a result of conformational averaging. This is the rationale for using different scaling factors for strong, medium, and weak NOEs. In addition, in small molecules the agreement should be considered as poor even if only one of the NOEs is severely violated. The steep decline of q_i with distance will decrease the overall index of agreement considerably in this case.

Results and Discussion

Bioactivity. Table II shows that the [D-Ala^{L2},L-Ala^{L5}]-EA is more effective in both GPI and MVD assays than analogs with 14-membered disulfide rings.³⁹ However, the ratio IC₅₀(MVD)/IC₅₀(GPI) is 0.882, indicating that the analog shows preference to neither μ nor δ opioid receptor subtype. In order to determine what conformational features of the molecule are responsible for such behavior, we performed a rigorous conformational analysis employing both NMR and molecular modeling.

NMR Data. All of the proton resonances were assigned using HOHAHA and ROESY experiments. Table II shows the chemical shifts observed for [D-Ala^{L2},L-Ala^{L5}]EA in DMSO solution. We note that the β protons on Ala^{L5} have the same chemical shift and appear as one slightly broadened peak in the spectrum. At the same time the β protons on D-Ala^{L2} are well separated, so that splittings on the α atom can be measured. We can deduce from this observation that, despite the fact that the D-Ala^{L2} and Ala^{L5} side chains are parts of the 13-membered ring, the side chain of Ala^{L5} may be much more flexible.

Measuring coupling constants allows one to estimate certain torsion angles in the molecule. Values of vicinal coupling constants $^3J_{\text{NH-C}_\alpha\text{H}}$ and $^3J_{\alpha\beta}$ are given in Table III together with corresponding torsions calculated from them. The values of the $^3J_{\alpha\beta}$ couplings for D-Ala^{L2} indicate that one of the conformers is greatly preferred, suggesting that the side chain in D-Ala^{L2} is constrained.

Temperature coefficients $\tau = d\delta/dT$ of the amide proton chemical shifts are presented in Table IV. It is generally known that temperature coefficients reflect the degree of solvent shielding. A low-temperature coefficient is usually considered as an indication of involvement in intramolecular hydrogen bonding. Most of the amide proton resonances in our analog are shifted upfield at elevated temperatures, with τ in the range of -4 to -8 ppb/K. For the Ala^{L5} amide, however, $\tau = -0.5$ ppb/K, indicating solvent shielding. Interestingly, Mosberg et al.³⁹ report very similar τ values for DPDPE in DMSO solution, with the residue D-Pen⁵ exhibiting temperature insensitivity

(38) Peishoff, C. E.; Dixon, J. S.; Kopple, K. D. Application of the distance geometry algorithm to cyclic oligopeptide conformation searches. *Biopolymers* 1990, 30, 45-56.

(39) Mosberg, H. I.; Haaseth, R. C.; Ramalingam, K.; Mansour, A.; Akil, H.; Woodard, R. W. Role of steric interactions in the delta opioid receptor selectivity of [D-Pen²,D-Pen⁵]enkephalin. *Int. J. Pept. Protein Res.* 1988, 32, 1-8.

Table III. Coupling Constants^a and Allowed ϕ and χ^1 Torsions for [D-Ala_L²,Ala_L⁵]EA

residue	³ J _{NH-C_αH}	³ J _{αβ¹}	³ J _{αβ²}	ϕ , deg	χ^1		
					f(t)	f(g ⁺)	f(g ⁻)
D-Ala _L ²	7.91	4.19	9.68	-60	0.145	0.209	0.646 ^c
				+80	0.646	0.209	0.145 ^c
				+160			
Gly	7.35 (1) ^b 3.48 (2) ^b			±67			
				±137			
Phe	8.43	5.48	8.05	-158	0.263	0.240	0.497 ^c
				-82	0.497	0.240	0.263 ^c
				+60			
Ala _L ⁵	9.09			-154			
				-86			

^a Values in hertz. ^b (1) is the proton resonating at lower field; (2) is the proton resonating at higher field. ^c These values were calculated using formulae given in Yamazaki and Abe (ref 26) and result in two interchangeable values for f(t) and f(g⁻), while f(g⁺) assumes one value only. Thus we obtain two alternative sets of population values.

Table IV. Temperature Coefficients for Amide Protons in [D-Ala_L²,L-Ala_L⁵]EA

residue	$-\tau = -d\delta/dT$ in ppb/K	residue	$-\tau = -d\delta/dT$ in ppb/K
Tyr (N-term)	1.5	Ala _L ⁵	0.5
D-Ala _L ²	4.0	CONH ₂ 1	4.5
Gly	4.0	CONH ₂ 2	4.5
Phe	7.5		

($\tau = 0.3$ ppb/K) similar to Ala_L⁵ in our molecule. We therefore conclude that the Ala_L⁵ amide in [D-Ala_L²,L-Ala_L⁵]EA is participating in intramolecular hydrogen bonding, most likely with the carbonyl oxygen of D-Ala_L² or Gly. We do not consider the carboxamide terminal oxygen to be the acceptor, since less solvent shielding and a higher τ value for Ala_L⁵ NH would then be expected, as the CONH₂ terminal group lies well outside the main 13-membered ring and is therefore more exposed to the solvent.

The NOE measurements constitute the most valuable structural data provided by NMR. We divided the NOEs observed in the ROESY experiment into three qualitative categories according to their intensity: strong, medium, and weak. A total of 5 strong, 13 medium, and 9 weak NOEs were observed and are indicated in Table V. As Table V shows, most of the NOEs observed are sequential or short-range NOEs. They cannot define the structure precisely, even in a cyclic molecule, providing only ranges of possible values for torsion angles. For instance, a medium NOE between the α proton of residue *i* and the amide proton of residue *i* + 1 may correspond to any value of ψ in residue *i* between +60° and 180°. In addition, no transannular NOEs were found that could have helped to identify an acceptor of the Ala_L⁵ amide hydrogen bond.

Distance Geometry Calculations. In order to find all possible conformations consistent with the NOE data, we performed a conformational search using the distance geometry algorithm, with distance constraints derived from observed NOEs. At the first stage of this search, NOEs to side chain protons were not used as constraints, since the resonances of prochiral β -protons cannot be assigned unambiguously. The NOEs with α -protons of Gly present a similar problem, and unlike the β -protons they are critical for determining the backbone conformation.

Of the two NOEs for Gly NH–Gly H¹_α and H²_α, we know that one is medium (separation of 2.5–3.0 Å) and the other is weak (separation of 3.0–4.0 Å). These possibilities lead to two conformations around Gly that can interconvert by

a rotation of approximately 60° about ϕ (Gly). The other ambiguous distance, Gly H_α–Phe NH, is then automatically determined.

By inspection of the molecule it is also evident that Ala_L⁵ NH may be hydrogen bonded to D-Ala_L² CO or to Gly CO. Two sets of constraints for the NOEs involving Gly α -protons together with two possible hydrogen bond constraints (the standard upper limit of 2 Å was used) resulted in four different sets of constraints that we used as input for distance-geometry calculations. From each set, 100 conformations were generated, most of which still had somewhat high potential energy but conformed to the given interatomic distance constraints and were free of severe steric overlaps.

Energy Minimizations and Selection of Best Conformations. All 400 conformations generated with the distance-geometry algorithm were then energy-minimized, resulting in 73 conformations within 10 kcal/mol of the lowest energy. Cluster analysis was performed to divide large numbers of structures into families of conformations based on similarity of backbone torsion angles. This procedure resulted in 34 clusters whose minimum-energy structures were within 10 kcal/mol of the lowest energy of all 400. The populations of these 34 clusters obtained ranged from 1 to 16; 6 major families with populations higher than 6 contained 64 structures. The large number of families indicates that even though [D-Ala_L²-L-Ala_L⁵]-EA is cyclic, it has considerable flexibility.

To select families of conformations that comply with our NOE data, we calculated observable parameters for each main cycle family and compared the calculated values with experimental data. These parameters include ϕ torsion angles, χ^1 for D-Ala_L², the distances from the Ala_L⁵ amide proton to potential hydrogen bond acceptors, and the overall index of NOE agreement Q.

The hierarchy of criteria applied to select best-fitting conformers can be summarized as follows: (1) potential energy within 10 kcal/mol above the lowest minimum found; (2) NOE index of at least 120 out of 140, implying agreement with both strong NOEs (Tyr H_α–D-Ala_L² HN and D-Ala_L² H_α–Gly HN); (3) presence of a hydrogen bond involving Ala_L⁵ NH as donor; and (4) maximum deviation of 20° for any single ϕ value from the coupling constant data. Cluster analysis allowed us to narrow the selection considerably because most conformers in a cluster meet these four basic requirements if the lowest energy member does, and conversely can be excluded if the lowest energy conformer violates one of them.

The three backbone ring conformers that comply best with the above criteria are shown in Table VI. Figure 4 shows structural plots of these conformations. Optimization of the side chains of Tyr and Phe was then performed by setting χ^1 (Tyr) and χ^1 (Phe) each to 180° (t), +60° (g⁺), and -60° (g⁻). Low-energy conformations with various combinations of side chain orientations are presented in Table VII.

Important Features of the Final Conformers. All of the conformations shown in Table VI have similar conformational strain, taken as the total potential energy minus the electrostatic energy. The three conformers all have the correct geometry for an Ala_L⁵-D-Ala_L² or Ala_L⁵-Gly transannular hydrogen bond. Unfortunately, there are no long-range transannular NOEs to show which of these two hydrogen bonds is formed, and therefore we consider both possibilities. In conformer A1 the Ala_L⁵

Table V. [D-Ala_L²,L-Ala_L⁵]EA: Nuclear Overhauser Effects^a

		Tyr				D-Ala _L ²				Gly			Phe					Ala _L ⁵			
		N	α	β	Ar	N	α	β ₁	β ₂	N	α ₁	α ₂	N	α	β ₁	β ₂	Ar	N	α	β	NH ₂
Ala _L ⁵	NH ₂																				M
	β						W	W												W	M
	α													W					W		
	N																				
Phe	Ar														S	M	M				
	β ₂												W		M						
	β ₁														S						
	α																				
	N																				
Gly	α ₂										M										
	α ₁										W										
	N																				
D-Ala _L ²	β ₂						W		S												
	β ₁								W												
	α						M		M												
	N																				
Tyr	Ar			S																	
	β			M	S																
	α			M																	
	N	M																			

^a S, strong; M, medium, W, weak.

Table VI. Summary of Properties of Final Backbone Conformations for [D-Ala_L²,L-Ala_L⁵]EA

properties	conformers		
	A1	A2	B
PE _{tot} ^a	-17.22	-15.50	-19.47
PE _{tot} - PE _{elec} ^b	+17.84	+14.96	+17.84
NOE index (Q)	131	136	139
max φ dev	18° (Gly)	16° (Gly)	7° (Gly)
H bond to Ala _L ⁵ c	D-Ala _L ² CO	Gly CO	Gly CO
ψ(Tyr) ^d	+163	+177	+162
φ(D-Ala _L ²)	+71	+165	+165
ψ(D-Ala _L ²)	-90	-162	-157
φ(Gly)	+49	+83	+74
ψ(Gly)	-94	-59	-84
φ(Phe)	-67	-83	-88
ψ(Phe)	-23	+44	+61
φ(Ala _L ⁵)	-69	-161	-80
ψ(Ala _L ⁵)	-17	+169	+46
χ ¹ (D-Ala _L ²)	+175	+177	-174
χ ² (D-Ala _L ²)	+126	+162	+165
χ ¹ (Ala _L ⁵)	+74	+55	-39

^a All energy values in kilocalories/mole. ^b The difference between total and electrostatic potential energy is an estimate of the conformational (bond, angle, and dihedral) strain. ^c Hydrogen bond from NH (donor) of first residue to CO (acceptor) of second. ^d All values for angles are in degrees.

amide is hydrogen bonded to the D-Ala_L² carbonyl oxygen, resulting in approximately a β-turn around Gly and Phe, and in A2 and B the Ala_L⁵ amide proton is hydrogen bonded to the Gly carbonyl oxygen, resulting in a γ-turn around Phe. In addition, conformations A2 and B have a γ-type turn around Gly. The torsion χ¹ for D-Ala_L² is trans for all three conformers, consistent with the coupling constant data. The maximum deviation of the φ torsions from the values predicted from coupling constants is -18°, which is within the limits originally set for the search.

Figure 4 shows structural plots of the three final conformers and indicates that two of these, A1 and A2, have one lanthionine bridge orientation while conformer B has a distinctly different array. One can refer to the Ala_L⁵ part of the sulfur bridge in these two types of structures as "down" (A1, A2) and "up" (B), though the difference is best represented by χ¹(Ala_L⁵) values: if χ¹(Ala_L⁵) is negative (roughly gauche⁻) the orientation is "up"; if positive (roughly gauche⁺), it is "down". Figure 4 shows

that while the D-Ala_L² and Gly backbone torsions are quite constrained, those around the Phe-Ala_L⁵ side of the ring are markedly flexible. Therefore, the conformational search has allowed us to find two major families of main cycle conformations consistent with the NMR data and two subfamilies within the A family (A1 and A2). Any single family may represent a preferred conformation, or all of them may coexist in equilibrium. Identical chemical shifts observed for the two Ala_L⁵ β protons support this suggestion. In order to explore the possibility that families A and B can interconvert, we carried out molecular dynamics simulations starting from conformers A1 and B.

Molecular Dynamics Simulations. To probe the possibility of a conformational equilibrium between families A1, A2, and B shown in Figure 4, we have carried out in vacuo molecular dynamics simulations at 300 K for a total time of 100 ps, starting from two different conformers, A1 and B. Figure 5 shows a superposition of the structures from the run starting with A1; from this we see two major qualitative features in the dynamics: the tyrosine portion is very flexible, as is the carboxy-terminal amide moiety, and the Phe-Ala_L⁵ region is the most flexible part of the 13-membered ring. A similar result is obtained when dynamics are started from conformer B.

In both dynamics runs we observed conformational transitions within the ring; the trajectories shown in Figures 6 and 7 give more quantitative information on these transitions. All three rotamers A1, A2, and B are observed to interconvert during the dynamics, no matter which starting conformer was chosen. As a rule each conformational transition included a simultaneous change in two torsion angles, as summarized in Table VIII. The A2 to B transition involves simultaneous rotation of two adjacent bonds around the α carbon of Ala_L⁵ (N-C_α and C_α-C_β). In the A1 to A2 transition, ψ(Phe) and φ(Ala_L⁵) change in concert, resulting in a flip of the plane of the peptide bond. The most interesting transition, however, is A1 to B, where the torsions separated by two bonds, ψ(Phe) and χ¹(Ala_L⁵), changes simultaneously. Interestingly, φ(Ala_L⁵) undergoes no significant shifts during the flips of the two torsions surrounding it: it is the pivotal point

Table VII. Side-Chain Conformations and Energies Derived from the Three Best Backbones Conformations of [D-Ala_L²,L-Ala_L⁵]EA

conformer A1				conformer A2				conformer B			
energy ^a	ψ(Tyr) ^b	χ ¹ (Tyr)	χ ¹ (Phe)	energy	ψ(Tyr)	χ ¹ (Tyr)	χ ¹ (Phe)	energy	ψ(Tyr)	χ ¹ (Tyr)	χ ¹ (Phe)
-17.22	+163	-178	+59	-15.50	+177	+62	+56	-19.55	-171	+69	+58
-15.72	+164	-178	-56	-15.18	+178	-170	-60	-19.48	+162	+180	-172
-15.41	+171	-60	+60	-14.30	+171	-178	-174	-19.29	+170	-173	-54
-14.49	+175	+63	-56	-13.94	+178	-60	+58	-17.82	+147	+172	+61
-13.89	-171	-61	-56	-13.06	+177	+62	-60	-17.06	-172	+71	-56
-13.78	+162	-178	-174	-12.53	+177	-61	-60	-16.42	+175	-62	+59
-13.47	+174	+62	+57	-10.83	+177	+62	-170	-15.14	-172	+70	-170
-11.97	+171	-60	-175	-9.92	+173	-177	+44	-14.56	+172	-60	-56
-9.96	+175	+63	-168	-9.92	+177	-60	-172	-12.55	+172	-61	-170

^a Energy values in kilocalories/mole. ^b Angle values in degrees.

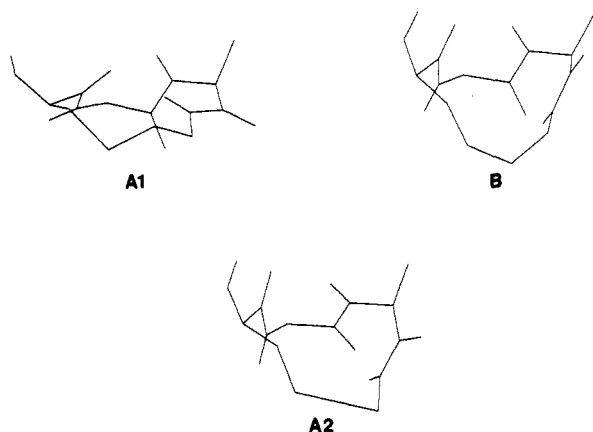


Figure 4. Structural drawings of the three conformers A1, A2, and B obtained after application of the distance geometry program, using NMR constraints, and energy minimization (see text). Upper left, A1; lower center, A2; upper right, B. Only the non-hydrogen atoms and amide protons in the main 13-membered ring are shown; the β-carbon of phenylalanine is also included to indicate the orientation of that side chain. This manner of presentation assists in visualizing the differences in 13-membered ring shape among these three families.



Figure 5. Superposition of structures of [D-Ala_L²,L-Ala_L⁵]EA resulting after every 10 ps of dynamics simulation, starting from conformer B in which χ¹(Ala_L⁵) = *g*. The starting equilibrated conformation and all frames up to 100 ps are shown (a total of 11 structures). Note that the lanthionine bridge and Phe backbone regions are much more flexible than is the region around Gly during the 100 ps of dynamics that were run; also, the Tyr aromatic ring is more mobile than the Phe ring. Initiation of dynamics from conformer A1 to A2 gives a similar result.

for this most frequently observed conformational transition. The values of the χ¹ angle in A1 and A2 (+40°) and in B (-30°) differ from the generally preferred χ¹ values of 180°, 60°, and -60°, because these torsions are part of a very constrained 13-membered ring.

We can therefore conclude that the dynamics simulations presented support our hypothesis that conformers found in the searches coexist in equilibrium in solution. Three linked torsions, ψ(Phe), φ(Ala_L⁵), and χ¹(Ala_L⁵),

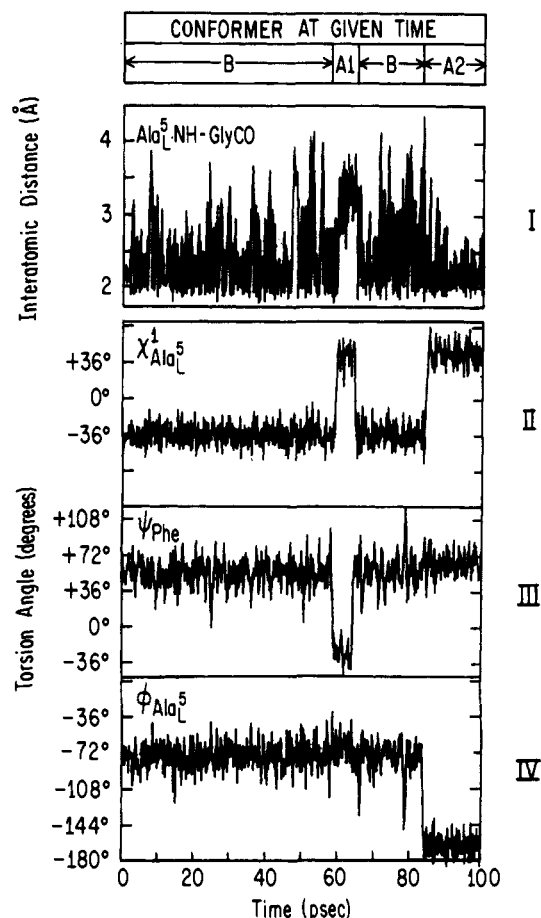


Figure 6. Traces of properties of the [D-Ala_L²,L-Ala_L⁵]EA molecule as a function of time during 100 ps of dynamics simulation, initiated from conformer B. The uppermost trace shows the distance from the Ala_L⁵ NH proton to the Gly CO oxygen; the second from the top, the torsion χ¹ of Ala_L⁵; the third, the torsion ψ of Phe; and the bottom trace, the torsion φ of Ala_L⁵. Comparing the torsions in the traces with those listed in Table V for the three conformer families A1, A2, and B, we can see that the starting conformer is B; at about 60 ps a transition to A1 occurs but reverts to B after about 5 more ps; at about 80 ps a second shift to A2 is seen.

contribute the most to the ring flexibility. Of these torsions, at least two must flip in concert in order to bring about a transition from one rotamer to another.

Comparing the traces for χ¹(Ala_L⁵), ψ(Phe) and the distance between the Gly carbonyl oxygen and the Ala_L⁵ amide proton, we see further that this interatomic separation correlates with the torsional flips: starting from the B rotamer, the Ala_L⁵-Gly distance shifts from an average of 3.0–3.2 Å to 2.0–2.1 Å, permitting hydrogen bond formation at the same time as χ¹(Ala_L⁵) undergoes

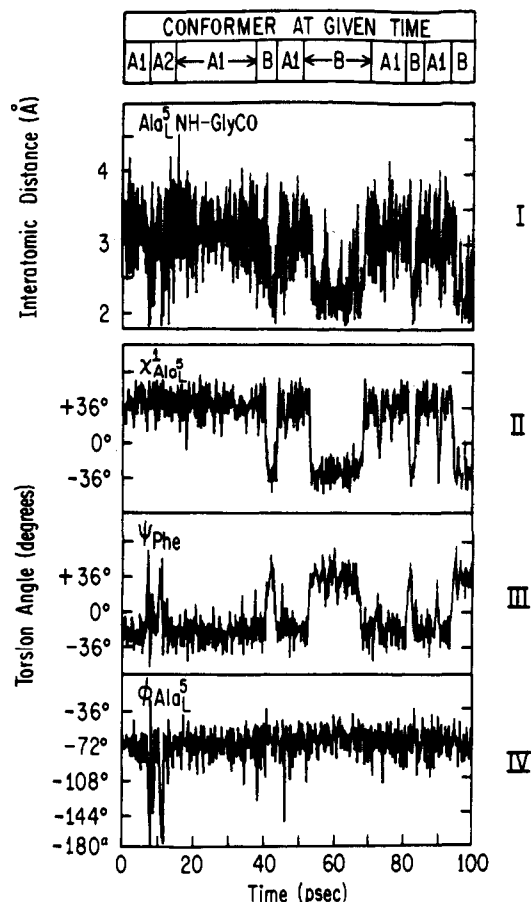


Figure 7. Dynamics traces similar to those in Figure 6, but initiated from conformer A1. It is evident from a comparison of Figures 6 and 7 that the three families can interconvert during dynamics simulations regardless of the starting conformation: very brief transitions between A1 and A2 occur at 10 and 15 ps, while transitions between A1 and B occur at 40, 55, 80, and 90 ps.

Table VIII. Summary of Torsional Transitions Occurring in Dynamics Simulations at 300 K

conformations	torsions	approx values
A1 → A2	$\psi(\text{Phe})$	$-30^\circ \rightarrow +60^\circ$
	$\phi(\text{Ala}_L^5)$	$-70^\circ \rightarrow -160^\circ$
A1 → B	$\psi(\text{Phe})$	$-30^\circ \rightarrow +40^\circ$
	$\chi^1(\text{Ala}_L^5)$	$+40^\circ \rightarrow -30^\circ$
B → A2	$\phi(\text{Ala}_L^5)$	$-70^\circ \rightarrow -160^\circ$
	$\chi^1(\text{Ala}_L^5)$	$-30^\circ \rightarrow +40^\circ$

the g^+ to g^- transition. Conversely, this hydrogen bond breaks very briefly when the (initial) A rotamer shifts to the B form. We note, however, that the Ala^{L5}-Gly distance oscillates with an average amplitude of roughly 0.5 Å so that even when the hydrogen bond is said to be "present" it is fact rapidly breaking and re-forming. From these results and our NMR temperature shift data, it would appear that the B rotamer is preferred over A1 in solution.

The torsions $\chi^1(\text{Tyr})$, $\chi^1(\text{Phe})$, and $\chi^1(\text{Ala}_L^2)$ remain essentially constant at their starting values throughout the dynamics, though rapid oscillations of as much as 20° occur at least every 1 ps. In an attempt to correlate these side chain χ 's with the lanthionine shifts discussed, $\chi^1(\text{Phe})$ was set at gauche⁺ instead of its original trans for the A1 and B rotamers and the dynamics runs were repeated for both rotamers. The transitions in the Phe and Ala^{L5} torsions remain essentially the same for both starting values of $\chi^1(\text{Phe})$; no systematic correlation of side-chain

orientation with main cycle flips can be made from these results. There is some evidence for concerted shifts on both sides of the lanthionine bridge, such as an increase in $\chi^1(\text{Ala}_L^5)$ from +40° to +90°, accompanied by a shift in $\psi(\text{Ala}_L^2)$ from -145° to -90° in one dynamics run. The tyrosine exocyclic torsions $\psi(\text{Tyr})$ and $\phi(\text{Ala}_L^2)$ show large rotations of up to 100°, though $\chi^1(\text{Tyr})$ remains stable; this results in large fluctuations in the distance, as much as 5 Å as measured from C_γ(Tyr) to C_γ(Phe), between the two aromatic rings.

We now summarize our results and their significance. It is evident that the 13-membered ring of our opioid is very constrained: the torsions $\chi^1(\text{Ala}_L^2)$, $\psi(\text{Ala}_L^2)$, $\phi(\text{Gly})$, $\psi(\text{Gly})$, and $\phi(\text{Phe})$ remain quite stable among our optimal minimized structures (Table VI) and during molecular dynamics. Although no methyl substituents are present on the D-Ala^{L2} β carbon to provide steric hindrance to rotations around the C_α-C_β and C_β-S bonds, this part of the ring is nonetheless constrained. Dynamics reveals that some local flexibility exists around residues 4 and 5 (Phe and Ala^{L5}) enabling pairs of torsions in this region to undergo concerted transitions. This small degree of flexibility does not influence the mutual orientations of the two aromatic rings, since the D-Ala^{L2}-Gly region is very constrained. The torsion $\psi(\text{Tyr})$ can vary independently of the Phe and Ala^{L5} torsions, with the result that although the flexibility of the main ring has been decreased, the distance between the aromatic rings is still highly variable and therefore no increase in selectivity has been achieved compared to [D-Cys²,Cys⁵]enkephalin (DCLCE). The lack of selectivity of our compound has been observed in in vitro μ and δ receptor binding assays performed in the laboratories of Schiller and Yaksh; our opioid exhibits an IC₅₀ ratio (MVD/GPI) of 0.882, although it has 400 times greater μ affinity and 20 times greater δ affinity than [Leu⁵]enkephalin.

We conclude from these observations that the flexibility of the main-chain ring itself does not affect selectivity. It remains to be determined what factors do influence selectivity in this class of cyclic opioids. One of the possibilities is that selectivity is influenced by energetics of rotation around the ψ angle of Tyr. This torsion angle determines the relative orientation of this residue and the ring. An analysis of in vitro biological binding data shows that δ-selectivity occurs not because δ-potency increases, but rather because μ-potency decreases. This tendency can be illustrated by the observations of Mosberg et al.⁴⁰ on a series of β-methylcysteine-containing cyclic enkephalin analogs. These compounds are of the type [D-Cys²,D-Pen⁵]EA with two, one, or no β-methyl substituents on the second residue. Their results show that the affinity for the δ receptor does not depend significantly on the β-methylation of the side chain of this residue. However, the μ receptor affinity is greatly influenced by methylation. They hypothesize that a (3R)-β-methyl group contributes an unfavorable steric interaction with the μ receptor, while a (3S)-β-methyl substituent has no appreciable effect. This putative μ steric hindrance becomes much worse for the β,β'-dimethyl analog (DPDPE).

An alternative explanation based on consideration of intramolecular, in contrast to intermolecular, interactions can be proposed. We suggest that methylation of the

(40) Mosberg, H. I.; Sobczyk-Kojiro, K.; Subramanian, P.; Crippen, G. M.; Ramalingam, K.; Woodard, R. W. *J. Am. Chem. Soc.* 1990, 112, 822-829.

β -carbon of the second residue at the *pro-R* position prevents the molecule from acquiring the conformation necessary for interaction with the μ receptor. Specifically, the rotation around ψ angle of Tyr is most influenced by these substitutions. Synthesis, biological, and structural studies on lanthionine enkephalins with a mono- or dimethylated β -carbon in D-Ala_L² are now under way in our laboratory. Methylation of Ala_L⁵ may also be interesting in view of our observations on the local flexibility of the Phe-Ala_L⁵ side of the ring, allowing us to constrain this region further.

Conclusions. We synthesized a novel opioid H-Tyr-

$\text{[D-Ala}_L\text{-Gly-Phe-Ala}_L\text{]-NH}_2$ which is cyclized through a lanthionine bridge, with Ala_L denoting each of the two amino acid ends joined by a monosulfide linkage. Data from NMR, conformational searches and molecular dynamics simulations have revealed three principal interconverting families of 13-membered-ring conformations. Transitions from one family to another require concerted

changes in two torsion angles in the region between Phe and Ala_L⁵, i.e. $\psi(\text{Phe})$, $\phi(\text{Ala}_L^5)$, and $\chi^1(\text{Ala}_L^5)$. A decrease in the backbone ring flexibility caused by reducing the ring size from 14 to 13 atoms may be responsible for super-high activity of the analog, but did not result in an increase in selectivity as might have been expected. We therefore conclude that factors other than backbone ring flexibility may determine δ vs μ selectivity in this class of molecules.

Acknowledgment. We thank the National Institutes of Health (Grant Nos. DK 15410 and GM 18694) for their support of this research. Also we acknowledge NIH S10RR 05799 which provided support for the acquisition of the Silicon Graphics IRIS 4D-340. We also thank Dr. Toshimasa Yamazaki for helpful advice and discussion, Dr. Peter Schiller of the Clinical Institute of Montreal for his in vitro measurements of bioactivity, and Dr. Tony Yaksh of the Department of Anesthesiology, University of California at San Diego.